JOURNAL OF THERMOPHYSICS AND HEAT TRANSFER
Vol. 23, No. 4, October–December 2009

Fourier and Diffusive Heat Transfer in Hypersonic Nitrogen Flows: State-to-State Approach

I. Armenise*
Consiglio Nazionale delle Ricerche, 70126 Bari, Italy
and
M. Capitelli† and S. Longo‡
Bari University, 70126 Bari, Italy

DOI: 10.2514/1.41991

Diffusive q_{wrec} and Fourier q_F components of heat transfer in hypersonic nitrogen flows are discussed. Three models of partially catalytic surfaces differing on the vibrational level(s) pumped by the heterogeneous recombination process are proposed: the ground vibrational state model, the last vibrational state model, and the diffuse vibrational state model. A noncatalytic surface is also considered for comparison. State-to-state gas-phase kinetics are coupled to the state-to-state gas–surface interaction. To investigate the effects of the different surface models and of the gas-phase kinetics, two test cases are considered, taking surface temperature and surface recombination probability as parameters. It is demonstrated that both chemical properties and fluid dynamic properties, such as the surface heat flux, are strongly affected by the state-to-state gas-phase kinetics and the heterogeneous recombination model.

Nomenclature

C_N	=	mass fraction of atomic nitrogen, ρ_N/ρ
C_v	=	mass fraction of the vth vibrational level, ρ_v/ρ
$c_v^{N_2}$, c_v^N	=	specific heats at constant volume
D_N	=	diffusion coefficient of nitrogen atoms in the mixture, $m^2 \cdot s^{-1}$
E^D	=	dissociation energy, J
f	=	stream function
h_v	=	enthalpy of the vth vibrational level, J
k	=	thermal conductivity coefficient, $kg \cdot m \cdot K^{-1} \cdot s^{-3}$
k_B	=	Boltzmann constant, $J \cdot K^{-1}$
m_N	=	atomic nitrogen mass, kg
m_v	=	vth vibrational-level mass, kg
N^*	=	nitrogen adatoms density, part $\cdot m^{-2}$
n_{N_2}, n_N	=	molecular nitrogen and the atomic nitrogen number densities, part $\cdot m^{-3}$
Pr	=	Prandtl number
p	=	pressure, $N \cdot m^{-2}$
q	=	heat flux, $W \cdot m^{-2}$
q_F	=	heat flux due to thermal conductivity (Fourier flux), $W \cdot m^{-2}$
$q_{T\text{jump}}$	=	heat flux due to temperature jump, $W \cdot m^{-2}$
$q_{w\text{rec}}$	=	heat flux due to heterogeneous recombination, $W \cdot m^{-2}$
Sc	=	Schmidt number
S_T	=	source term of the energy equation
S_v	=	source terms of the continuity equations
T	=	temperature, K
T_e	=	temperature at the boundary-layer edge, K
T_g	=	gas temperature at the surface, K
T_w	=	surface temperature, K
v, w	=	species indices
v_{N_2}, v_N	=	molecular and atomic nitrogen thermal velocities, $m \cdot s^{-1}$
γ_v	=	surface recombination probabilities
ε_{rot}	=	rotational energy, J
$\varepsilon_{\text{vib}}^v$	=	vibrational energy, J
η	=	coordinate normal to the surface
θ	=	T/T_e
ρ	=	total density, $kg \cdot m^{-3}$
ρ_N, ρ_{N_2}	=	N, N_2 densities, $kg \cdot m^{-3}$
ρ_v	=	density in the vth vibrational level, $kg \cdot m^{-3}$

Subscripts

e	=	external edge of the boundary layer
w	=	wall

Received 4 November 2008; revision received 30 April 2009; accepted for publication 4 May 2009.

*Researcher, Istituto di Metodologie Inorganiche e dei Plasmi, Via Amendola 122/D; iole.armenise@ba.imip.cnr.it.

†Full Professor, Chemistry Department, Via Orabona 4; Istituto di Metodologie Inorganiche e dei Plasmi, Consiglio Nazionale delle Ricerche, 70126 Bari, Italy; mario.capitelli@ba.imip.cnr.it. Associate Fellow AIAA.

‡Full Professor, Chemistry Department, Via Orabona 4; Istituto di Metodologie Inorganiche e dei Plasmi, Consiglio Nazionale delle Ricerche, 70126 Bari, Italy; savino.longo@ba.imip.cnr.it.

I. Introduction

CHEMICAL–PHYSICAL models of hypersonic flows have been widely investigated to characterize the complex phenomenology occurring during reentry of vehicles into planetary atmospheres. After the shock, molecules in both vibrationally and electronically excited states and atoms in excited electronic states are formed and diffuse through the boundary layer interacting with the surface. Moreover, atoms recombining on the surface produce vibrationally and electronically excited molecules. Large improvement has been achieved in describing the coupling between vibration and dissociation/recombination processes by using multitemperature and state-to-state approaches [1–3]. Electronically excited states are either ignored or transformed in vibrationally excited molecules [4,5]. As an example, in gas-phase recombination of atomic nitrogen, the formed $N_2(A^3\Sigma_u^+)$ is transformed in a molecule in the ground-state vibrationally excited level of quantum number $v = 25$ [5].

The interaction of vibrationally excited molecules with surfaces and the formation of vibrationally excited molecules from the catalytic recombination of atomic species are generally ignored. Both processes are actively investigated nowadays by molecular dynamics (MD). The main results of MD [6–8] can be summarized as follows:

1) The accommodation of vibrational energy on the (ceramic) surfaces is generally small and depends on the vibrational quantum number.

2) The recombination of atomic species on the surfaces results in the formation of a long plateau in the vibrational distribution function of desorbed molecules, especially if the recombination process follows the Eley–Rideal mechanism.

MD results strongly depend on the potential energy surface entering in quasi-classical or quantum dynamic equations so that existing results can be used as a judicious guide to build realistic models to be inserted in fluid dynamic codes.

In regard to the vibrational distribution function created by the heterogeneous recombination process, we can essentially consider three models: 1) the ground vibrational state (GVS) model, 2) the last vibrational state (LVS) model, and 3) the diffuse vibrational state (DVS) model.

According to the GVS model, the surface recombination desorbs ground-state molecules (i.e., molecules in the first vibrational level $v = 0$) so that all of the recombination energy heats the surface, whereas the LVS model considers desorbed molecules in the last vibrational level. The recombination energy in this case is transported out from the surface. Finally, the DVS model spreads the recombination energy over the whole vibrational manifold of the desorbed molecules. Cases a and b can be considered to be two extreme conditions at the same level of the well-known catalytic (CS) and noncatalytic surface (NCS) for the recombination process.

The three models should strongly affect the heat transfer to the body. In particular, one expects that the LVS model should decrease the heat transfer to the surface as compared with the GVS model. The DVS results are between the LVS and GVS models. The situation, however, is not so simple. The superexcited vibrational molecules deriving from the LVS model, entering in the boundary layer of the reentering body, will be submitted to the gas-phase vibrational kinetics. Gas-phase relaxation of the superexcited molecules will, in any case, modify the temperature gradient in the boundary layer and, therefore, the Fourier component of the heat transfer (q_F). Briefly, q_F and diffusive $q_{w\mathrm{rec}}$ components are strongly coupled, giving rise to an unexpected behavior of the total heat transfer to the surface.

The aim of this paper is to describe this coupling by using the state-to-state model for both gas-phase and gas–surface interaction.

In this paper, Sec. II describes our boundary-layer model including fluid dynamics and chemical kinetics. Section II also presents the models for the calculation of the heat flux on the surface. Section III discusses results for a N_2–N mixture for two different flow conditions, comparing results obtained by the LVS, DVS, GVS, and NCS models.

II. Model

The coupling of fluid dynamics and chemical kinetics in hypersonic boundary layers has been widely discussed by the authors of this paper in other papers [9–11]. Briefly, we insert state-to-state kinetics in a 1-D system of boundary-layer equations in the Lees–Dorodnitsyn coordinates [5,9,10,12]. For the system under consideration (nitrogen in the dissociation/recombination regime), we can write the following system of second-order differential equations:

$$\frac{\partial^2 C_v}{\partial \eta^2} + (f \times Sc)\frac{\partial C_v}{\partial \eta} = S_v, \qquad v = 0\text{–}68 \tag{1a}$$

$$\frac{\partial^2 \theta}{\partial \eta^2} + (f \times Pr)\frac{\partial \theta}{\partial \eta} = S_T \tag{1b}$$

The first 69 equations are continuity equations for the 68 N_2 vibrational-level concentrations and atomic nitrogen concentration, and Eq. (1b) describes the temperature profile in the boundary layer. Sc and Pr are the Schmidt and Prandtl numbers, approximated by constant values: $Sc = 0.49$ and $Pr = 0.71$. This assumption, in line with the simplified fluid dynamics used in this work, could be improved by including multicomponent diffusion coefficients in the boundary-layer equations. The stream function is f. S_v and S_T are the source terms that take into account the vibration–vibration (VV), vibration–translation due to molecule–molecule collisions (VTm), vibration–translation due to molecule–atom collisions (VTa), and dissociation/recombination kinetic processes:

$$\begin{gathered} \mathrm{N_2}(v) + \mathrm{N_2}(w) \leftrightarrow \mathrm{N_2}(v-1) + \mathrm{N_2}(w+1) \\ \mathrm{N_2}(v) + \mathrm{N_2} \leftrightarrow \mathrm{N_2}(v-1) + \mathrm{N_2}, \qquad \mathrm{N_2}(v) + \mathrm{N} \leftrightarrow \mathrm{N_2}(w) + \mathrm{N} \\ \mathrm{N_2}(v) + \mathrm{N} \leftrightarrow \mathrm{N} + \mathrm{N} + \mathrm{N} \end{gathered} \tag{2}$$

The dissociation/recombination processes due to molecule–molecule collisions are taken into account by the ladder-climbing model. In this model, atoms are considered as molecules in a pseudovibrational level, located just above the last bound vibrational level of the molecule. Dissociation/recombination processes are described by VV and VTm processes involving this pseudolevel. It is worth noting that atom–molecule collisions involve both monoquantum and multiquantum transitions, whereas only monoquantum transitions are considered for molecule–molecule interactions.

In regard to the boundary conditions, we assume chemical and vibrational equilibrium at T_e (that is, the temperature of the boundary external edge), and we fix the surface temperature T_w. Moreover, we assume the following mass fraction gradients [11]:

$$\left.\frac{\partial C_{\mathrm{N}}}{\partial \eta}\right|_w = \frac{\sum_v \gamma_v}{D_{\mathrm{N}}}\sqrt{\frac{k_B T}{2\pi m_{\mathrm{N}}}}\cdot C_{\mathrm{N}} \qquad \left.\frac{\partial C_{\mathrm{N_2}}(v)}{\partial \eta}\right|_w = -\frac{\gamma_v}{D_{\mathrm{N}}}\sqrt{\frac{k_B T}{2\pi m_{\mathrm{N}}}}\cdot C_{\mathrm{N}} \tag{3}$$

where γ_v is the recombination probabilities of state selective surface recombination reaction

$$\mathrm{N} + \mathrm{N} + \mathrm{wall} \rightarrow \mathrm{N} + N^* \xrightarrow{\gamma_v} \mathrm{N_2}(v) + \mathrm{wall} \tag{4}$$

and N^* represents the adatoms: that is, atoms previously adsorbed by the surface. When the surface is chosen as noncatalytic and nondeactivating (NCS model), the mass fraction gradients are set equal to zero.

The total heat flux in the boundary layer consists of a term due to thermal conductivity (the Fourier component), a term due to mass diffusion, a term due to thermal diffusion [12–14], and a term due to diffusion of vibrational energy [11,15–17]. These terms depend, respectively, on the gradients of temperature, pressure, chemical species molar fractions, and vibrational-level populations.

To a first approximation, the heat flux to the surface can be expressed by the sum of a thermal conduction term and a diffusion term [18]:

$$q_w = -k\left.\frac{\partial T}{\partial y}\right|_w - \Sigma_V\left(E_V \gamma_V n_{\mathrm{N}}\sqrt{\frac{K_B T}{2\pi m_v}}\right) \tag{5}$$

The first term of Eq. (5) is the Fourier term. The Fourier heat flux is generally a good approximation of the thermal conduction heat flux provided the temperature slip condition is considered; that is, the gas rarefaction is taken into account as a temperature jump on the surface.

In the transition regime that holds in the range of 150–92 km of altitude [12], the flow can still be studied using the continuum flow equations, but the velocity no-slip and temperature no-slip boundary conditions fail. One should take into account that the flow velocity at the surface, due to low gas density, is no longer zero but has a finite value (velocity slip condition). Analogously, the gas temperature at the surface must be taken differently from the surface temperature (temperature slip condition).

Actually, this is an approximate way to take into account the Knudsen layer in the transition regime. A more rigorous way to take into account the Knudsen layer is to solve the Boltzmann equation in the Knudsen layer [19,20].

At this stage, the temperature slip condition (that is, the temperature jump between the gas temperature at the surface T_g and the surface temperature T_w) must be implemented. Méolans and Dadzie [21] calculated the temperature jump assuming that the heat flux entering the Knudsen layer, given by a Fourier law as at the limit of the validity of the continuum model, is equal to the heat flux in contact with the wall. This assumption is possible if the effects of the gaseous particle collisions inside the Knudsen layer are neglected; that is, both the particle distribution functions and macroscopic gradients at the point of contact on the wall coincide with the corresponding quantities at the entrance of the Knudsen layer. Following the Méolans and Dadzie assumption, we write

$$q_{T\text{jump}} = q_F \tag{6}$$

where $q_{T\text{jump}}$ is the heat flux in contact with the wall and q_F is the Fourier heat flux entering the Knudsen layer. From a microscopic point of view, an approximate expression for the thermal conduction heat flux to the surface can be obtained; this expression is based on the hypothesis that the flux of molecules through the Knudsen layer is effusive and that, following effusion, any particle thermalizes locally. This simplified view is supported by the fact that the layer width is comparable with the mean free path [22]. We can therefore write

$$q_{T\text{jump}} = (T_g - T_w)\left(c_v^{\mathrm{N}_2} n_{\mathrm{N}_2} \frac{v_{\mathrm{N}_2}}{4} + c_v^{\mathrm{N}} n_{\mathrm{N}} \frac{v_{\mathrm{N}}}{4}\right) \tag{7}$$

where $c_v^{\mathrm{N}_2}$ and c_v^{N} are the specific heats at constant volume, n_{N_2} and n_{N} are the molecular nitrogen and the atomic nitrogen number densities, and v_{N_2} and v_{N} are the molecular and atomic nitrogen thermal velocities:

$$v_M = \sqrt{\frac{8k_BT}{\pi m_M}}, \qquad M = \mathrm{N}_2, \mathrm{N}$$

By comparing Eqs. (6) and (7) the following expression for the temperature jump $(T_g - T_w)$ is obtained:

$$(T_g - T_w) = q_F \Big/ \left(c_v^{\mathrm{N}_2} n_{\mathrm{N}_2} \frac{v_{\mathrm{N}_2}}{4} + c_v^{\mathrm{N}} n_{\mathrm{N}} \frac{v_{\mathrm{N}}}{4}\right) \tag{8}$$

T_g is then inserted both in the boundary conditions and in the thermal velocities calculation on the wall.

The second term of Eq. (5) is the equivalent of the mass diffusion term of the heat flux formula in the boundary layer.

In the frozen boundary layer, the heat flux is not affected by the diffusion. Only the particles impinging the surface and reacting there affect the heat flux. The others are just reflected by the surface; therefore, their gradients are zero. In Eq. (5), only recombination processes [see Eq. (4)] have been taken into account on the surface. The energy balance of the recombination reaction (4) is

$$\begin{aligned}\Delta E &= 2E_{\mathrm{N}} - E_{\mathrm{N}_2} = 2\left(\frac{E^D}{2} + \frac{3}{2}k_BT\right) - \left(\varepsilon_{\text{rot}} + \varepsilon_{\text{vib}}^v + \frac{3}{2}k_BT\right) \\ &= \left(E^D + \frac{3}{2}k_BT - \varepsilon_{\text{rot}} - \varepsilon_{\text{vib}}^v\right)\end{aligned} \tag{9}$$

The energy released to the surface is proportional to this energy balance, so that in the state-to-state approach, the second term of the heat flux [Eq. (5)] (that is, the heat flux due to recombination on the surface) can be written as

$$q_{w\text{rec}} = \Sigma_v\left(\gamma_v n_{\mathrm{N}} \frac{v_{\mathrm{N}}}{4}\frac{1}{2}\left(E^D + \frac{3}{2}k_BT - \varepsilon_{\text{rot}} - \varepsilon_{\text{vib}}^v\right)\right) \tag{10}$$

where $q_{w\text{rec}}$ depends on the number of nitrogen atoms n_{N} impinging the surface at thermal velocity v_{N}, on their state selected surface recombination probability γ_v, and on the energy released to the surface.

In the limit cases of the GVS and LVS models, ΔE assumes the following forms:

$$(\Delta E)_{\text{GVS}} \approx (E^D + \tfrac{3}{2}k_BT - \varepsilon_{\text{rot}}) \tag{11}$$

$$(\Delta E)_{\text{LVS}} \approx (\tfrac{3}{2}k_BT - \varepsilon_{\text{rot}}) \tag{12}$$

The diffusive terms, respectively, become

$$(q_{w\text{rec}})_{\text{GVS}} \approx \frac{1}{2}\left(\gamma_0 n_{\mathrm{N}} \frac{v_{\mathrm{N}}}{4}\left(E^D + \frac{3}{2}k_BT - \varepsilon_{\text{rot}}\right)\right) \tag{13}$$

$$(q_{w\text{rec}})_{\text{LVS}} \approx \frac{1}{2}\left(\gamma_{\text{last}} n_{\mathrm{N}} \frac{v_{\mathrm{N}}}{4}\left(\frac{3}{2}k_BT - \varepsilon_{\text{rot}}\right)\right) \tag{14}$$

As a consequence, the following inequality holds:

$$(q_{w\text{rec}})_{\text{GVS}} \gg (q_{w\text{rec}})_{\text{LVS}} \tag{15}$$

The results obtained by adopting the presented models will be discussed in detail in the next section. However, before ending this section, it is interesting to observe (Table 1) the effect of the temperature jump on $q_{w\text{rec}}$ and q_F. In Table 1, $q_{w\text{rec}}$ and q_F obtained considering the temperature slip boundary condition (i.e., including the temperature jump) and considering the temperature no-slip boundary condition (i.e., neglecting the temperature jump) are reported. All of the gas-phase processes [see Eq. (2)] have been included in these test cases. Four different surface recombination models (NCS, GVS, DVS, and LVS) have been used. The values of input parameters for this test case are $T_w = 1000$ K, $T_e = 5950$ K, $P_e = 10^4$ N/m^2, $\beta = 10^4$ s^{-1}, and $\gamma = 5 \times 10^{-2}$. The results have been reported in Table 1. Inspection of this table shows that the maximum deviation between slip and no-slip conditions is 20.3% for $q_{w\text{rec}}$ in the DVS model.

III. Results

The heat flux due to recombination on the surface has been investigated by running the 1-D boundary-layer code considering different surface temperatures ($T_w = 300$, 500, 1000, 1500, and 2000 K) and four models for the surface catalycity: NCS; CS in which atoms recombine on the first ($v = 0$) vibrational level of the molecule (GVS); CS in which atoms recombine on the whole vibrational energy ladder (DVS): that is, the recombination process pumps each vibrational level (a further assumption is made on γ_v

Table 1 Values[a] of $q_{w\text{rec}}$ and q_F close to the surface in the case $T_w = 1000$ K, $T_e = 5950$ K, $P_e = 10^4$ N/m^2, $\beta = 10^4$ s^{-1}, and $\gamma = 5 \times 10^{-2}$ and for different surface recombination models

	Boundary condition[b]	NCS	GVS	DVS	LVS
$q_{w\text{rec}}$, W/m^2	Temperature slip	0	1.7841×10^5	1.3161×10^5	13,377
$q_{w\text{rec}}$, W/m^2	Temperature no-slip	0 (0%)	1.9149×10^5 (7.3%)	1.5840×10^5 (20.3%)	12,509 (6.5%)
q_F, W/m^2	Temperature slip	6.6750×10^5	5.0030×10^5	1.0950×10^6	9.4410×10^5
q_F, W/m^2	Temperature no-slip	7.4170×10^5 (11.1%)	5.2530×10^5 (5%)	1.1780×10^6 (7.6%)	9.8690×10^5 (4.5%)

[a]All of the gas-phase kinetic processes have been included in the calculations.
[b]The temperature jump has been either considered (temperature slip boundary condition) or neglected (temperature no-slip condition).

which is obtained by spreading the full recombination coefficient on the different levels with the same weight); and CS in which atoms recombine on the last vibrational level of the molecule (LVS).

A first set of test cases has been run with the following boundary conditions and input parameters: $T_e = 5950$ K, $P_e = 10^4$ N/m^2, β (that is, the inverse of the residence time of a fluid element in the boundary layer) has a value of 10^4 s^{-1}, and $\gamma = 0.05$. This choice, loosely matching reentry conditions, gives us the possibility of comparing the present results with those obtained by Armenise et al. [23]. Moreover, to better understand the results, the test cases have been run both including and neglecting the state-to-state kinetics in gas phase.

First, we discuss the behavior of vibrationally excited molecules and atomic nitrogen concentration near the surface ($\eta = 0$). The trend of atomic nitrogen density versus the surface temperature is reported in Figs. 1a and 1b. In particular, the results of Fig. 1a have been calculated by including the state-to-state kinetics in gas phase, and the corresponding results of Fig. 1b have been calculated by neglecting the state-to-state kinetics in gas phase. The results strongly depend on the recombination model used. In the case of Figs. 1a and 1b, the assumption of noncatalytic surface leads to the highest concentration of atomic nitrogen near the surface. In the presence of gas-phase kinetics, the LVS assumption yields a nitrogen concentration close to that obtained with the NCS assumption. This is due to the redissociation of the gas molecules from the last bound vibrational level. Conversely, neglecting gas-phase state-to-state kinetics strongly affects the LVS results. In this case, the nitrogen atom density strongly decreases with respect to the corresponding results of Fig. 1a; indeed, no redissociation of the last vibrational level occurs. In Figs. 1a and 1b, the results of the GVS model present the lowest atomic nitrogen concentration, and the DVS approximation results are between the LVS and GVS values.

Regarding the molecular nitrogen density near the surface, similar considerations can be given. Taking into account that n_N and n_{N_2} depend on the surface model in an opposite way, the concentration of N_2 increases passing from NCS to LVS, then to DVS, and finally to the GVS model. Another observation is that n_{N_2} and n_N decrease when increasing T_w.

Figures 2a and 2b show the corresponding vibrational distributions (VDs) near the surface with (Fig. 2a) and without (Fig. 2b) gas-phase kinetics. In the presence of gas kinetics, all models (NCS, GVS, LVS, and DVS) yield very structured VDs.

The reported differences are due to the combined effects of the surface model and of the gas-phase kinetics: in particular, the homogeneous recombination. Near the surface, the atomic nitrogen concentration is higher in the NCS model than in the GVS model, causing a stronger gas-phase recombination: that is, higher pumping of the vibrational energy and more populated vibrational distributions. Large differences are also present in the vibrational distributions arising from the LVS and DVS models (Fig. 2a). In particular, the LVS model presents a long plateau and a strong peak on the last vibrational level. The peak is due to the preferential surface recombination model. The plateau is due to the gas-phase recombination and the redistribution of the molecular vibrational states through the VV and VT processes. Finally, the DVS model presents a very smooth VD with a long plateau, which is higher than the plateau of the LVS model because of the spread of the heterogeneous recombination on the whole vibrational ladder.

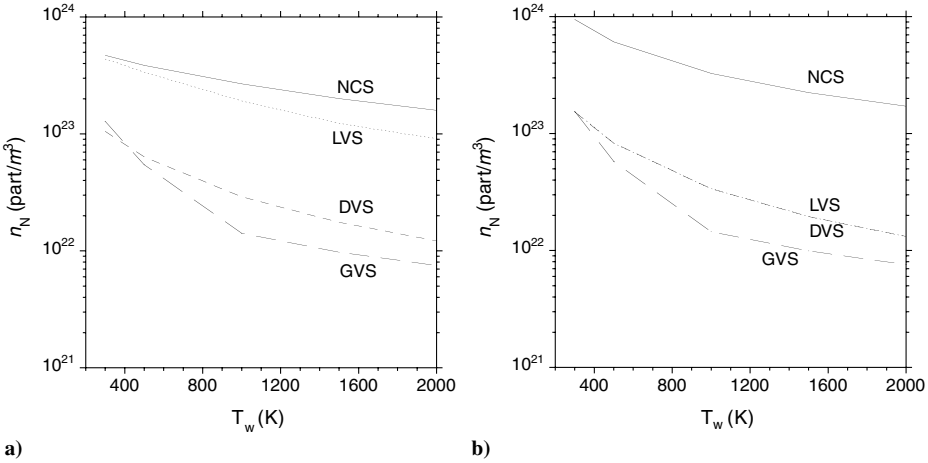

Fig. 1 Atomic nitrogen close to the surface number densities obtained either a) including or b) neglecting the gas-phase kinetics of Eq (2); $T_e = 5950$ K, $P_e = 10^4$ N/m^2, $\beta = 10^4$ s^{-1}, and $\gamma = 5 \times 10^{-2}$.

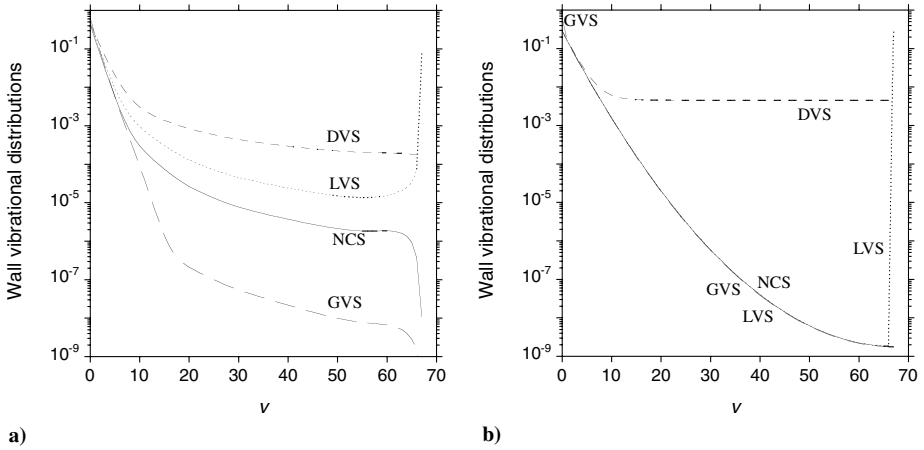

Fig. 2 Surface vibrational distributions versus the vibrational level obtained either a) including or b) neglecting the gas-phase kinetics of Eq. (2); $T_w = 1000$ K, $T_e = 5950$ K, $P_e = 10^4$ N/m^2, $\beta = 10^4$ s^{-1}, and $\gamma = 5 \times 10^{-2}$.

Neglecting the gas-phase kinetics (Fig. 2b), the vibrational distributions obtained using the NCS and GVS models practically coincide for $v > 0$, showing a Boltzmann distribution. Differences are indeed present on $v = 0$. The same situation occurs for the LVS model, with the exception of the sharp peak on $v = 67$. It is interesting to stress that in the NCS model, the flow is frozen and the Boltzmann distribution from the boundary-layer edge reaches the surface in the absence of gas-phase kinetics. Conversely, the vibrational distribution obtained with the DVS model presents a long plateau, due to the heterogeneous recombination distributed on all the vibrational levels.

It should be noted that the differences coming from the four models persist along the boundary layer. This point can be understood by inspection of Figs. 3a and 3b, in which the concentrations of atomic nitrogen have been plotted as a function of η (remember that $\eta = 0$ is the surface and $\eta = 8$ is the edge of the boundary layer).

There are two main differences between the case in which gas-phase kinetics are included and the case in which it is neglected. The first is represented by ρ_N/ρ in the LVS model. In the LVS model, when gas-phase kinetics are considered (Fig. 3a), the molecules recombined at the wall on the last vibrational level easily redissociate due to gas-phase kinetics, and then the atomic mass fraction increases again. As a consequence, the atomic mass fraction when gas-phase kinetics are included is about one magnitude order higher than in the case in which gas-phase kinetics are neglected (Figs. 3a and 3b). The second important difference is related to the NCS model, in which ρ_N/ρ is constant along the boundary layer when kinetics are frozen and the unchanged external flow reaches the surface. The ρ_N/ρ ratio slowly decreases toward the surface, due to the gas-phase recombination when kinetics are allowed. In the DVS and GVS models, the surface recombination overcomes the gas-phase dissociation/recombination processes; the ρ_N/ρ profiles do not differ too much whether gas-phase kinetics are included or not.

Let us now examine heat flux due to the recombination of atomic nitrogen according to the GVS, LVS, and DVS models (i.e., the term $q_{w\mathrm{rec}}$). One can expect that the surface heat flux should present lower values for the LVS model and higher values for the GVS model. The results obtained with the DVS model are between the LVS and GVS values. Moreover, state-to-state gas-phase kinetics should affect the LVS results for the reasons previously discussed. This can be appreciated by observing Figs. 4a and 4b, in which the surface heat flux calculated according to the different assumptions is reported as a function of the surface temperature. In any case, the heat flux calculated by using the LVS assumption presents lower values that are also strongly affected by state-to-state gas-phase kinetics. It is also interesting to observe that with the wall temperature increasing, $q_{w\mathrm{rec}}$ increases in the LVS model case, whereas it decreases in the DVS and GVS model cases. This behavior is due to the behavior of the different factors, with their different weights, in $q_{w\mathrm{rec}}$ [see Eq. (10)]. The thermal velocity v_N increases with T_w. Conversely, the atomic nitrogen density n_N decreases with T_w, as already shown in Fig. 1. Moreover, n_N depends on the surface model passing from its

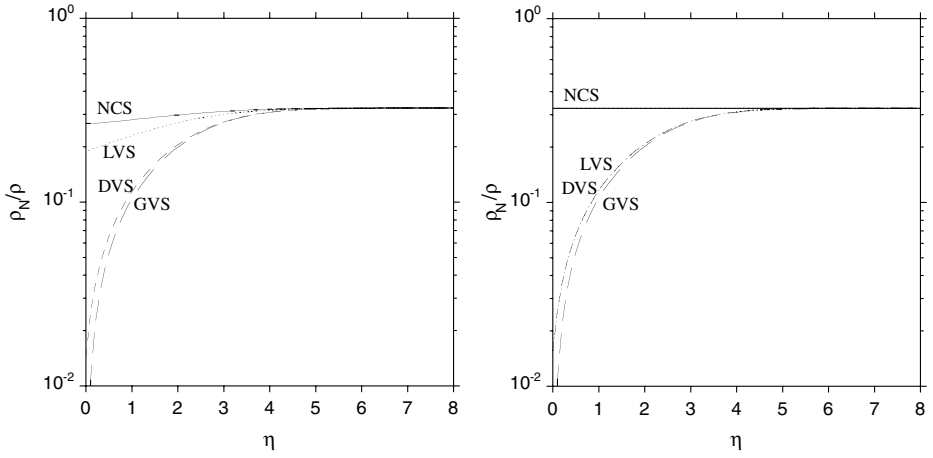

Fig. 3 Atomic and molecular mass fractions versus normal to the surface η obtained either a) including or b) neglecting the gas-phase kinetics of Eq. (2); $T_w = 1000$ K, $T_e = 5950$ K, $P_e = 10^4$ N/m^2, $\beta = 10^4$ s^{-1}, and $\gamma = 5 \times 10^{-2}$.

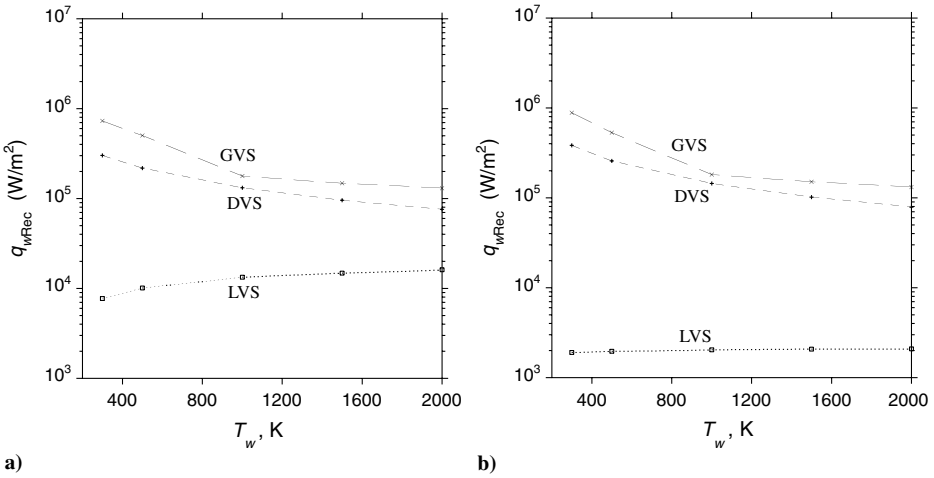

Fig. 4 Heat flux due to the surface recombination versus the surface temperature T_w obtained either a) including or b) neglecting the gas-phase kinetics of Eq. (2); $T_e = 5950$ K, $P_e = 10^4$ N/m^2, $\beta = 10^4$ s^{-1}, and $\gamma = 5 \times 10^{-2}$.

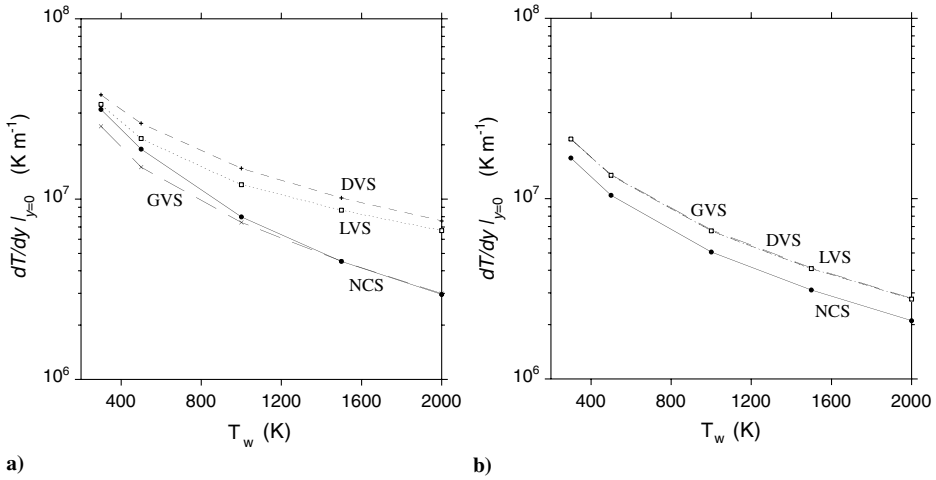

Fig. 5 Temperature gradient on the surface versus the surface temperature T_w obtained either a) including or b) neglecting the gas-phase kinetics of Eq. (2); $T_e = 5950$ K, $P_e = 10^4$ N/m^2, $\beta = 10^4$ s^{-1}, and $\gamma = 5 \times 10^{-2}$.

higher value (corresponding to the NCS model) to its lower value (corresponding to GVS model) through the LVS and DVS models. In the energy-balance term [Eqs. (9) and (10)], the translational and rotational energies increase with T_w. The vibrational and formation energies do not depend on T_w. Translational and rotational terms are important in the LVS model, thus determining the increase of $q_{w\mathrm{rec}}$ with T_w (Fig. 4). On the other hand, these contributions are not important in the other two models (GVS and DVS), in which $q_{w\mathrm{rec}}$ decreases as a function of T_w (Fig. 4).

Let us now examine the Fourier component of the heat flux, which strongly depends on the temperature gradient. This quantity, which has been reported in Figs. 5a and 5b, depends on the different surface models as well as on the gas-phase kinetics. We can expect that the surface recombination on the last vibrational level and the diffuse

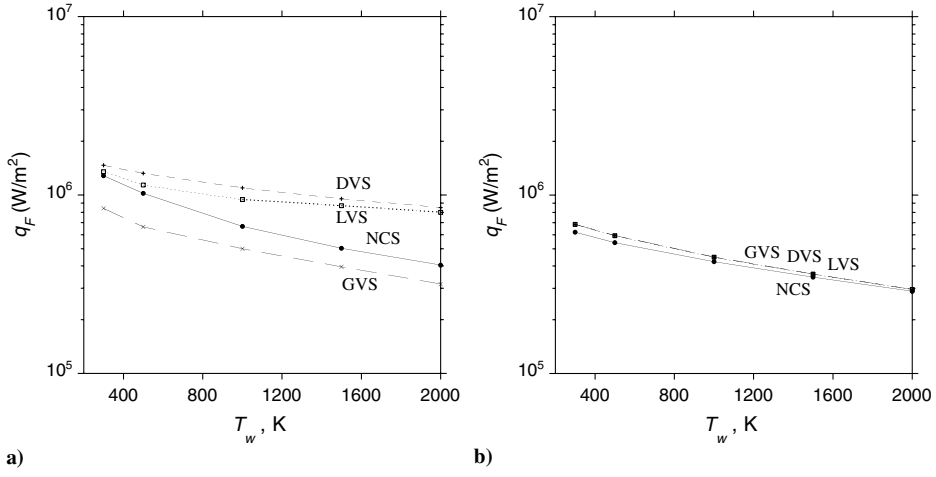

Fig. 6 Fourier heat flux on the surface versus the surface temperature T_w obtained either a) including or b) neglecting the gas-phase kinetics of Eqs. (2); $T_e = 5950$ K, $P_e = 10^4$ N/m^2, $\beta = 10^4$ s^{-1}, and $\gamma = 5 \times 10^{-2}$.

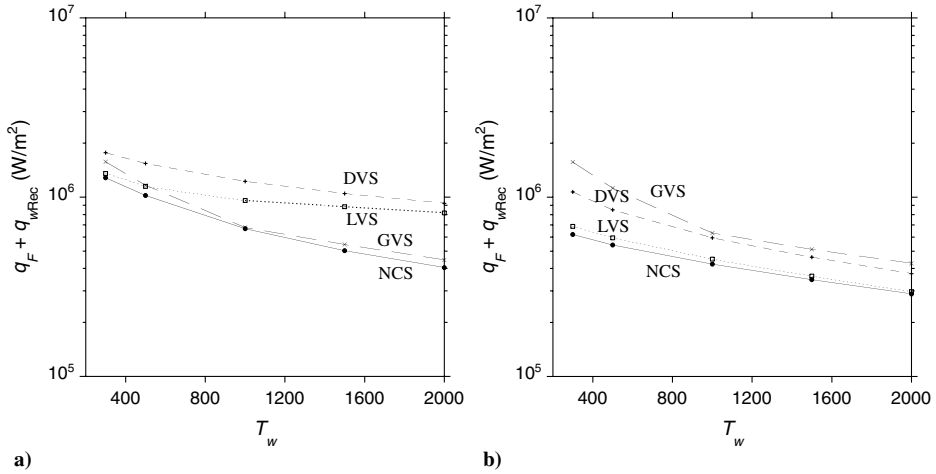

Fig. 7 Heat flux on the surface versus the surface temperature T_w obtained either a) including or b) neglecting the gas-phase kinetics of Eq. (2); $T_e = 5950$ K, $P_e = 10^4$ N/m^2, $\beta = 10^4$ s^{-1}, and $\gamma = 5 \times 10^{-2}$.

Table 2 Present work ($q_{wrec} + q_F$) values[a] as well as Armenise et al. [23] heat fluxes on the surface for different surface models with $T_e = 5950$ K, $P_e = 10^4$ N/m^2, $\beta = 10^4$ s^{-1}, and $\gamma = 5 \times 10^{-2}$

	Present work q_{wrec} $+q_F$ W/m^2	Heat flux [23],W/m^2	Present work $q_{wrec} + q_F$ W/m^2	Heat flux [23], W/m^2	Present work q_{wrec} $+q_F$ W/m^2	Heat flux [23], W/m^2
T_w, K	NCS	NCS	GVS	GVS	LVS	Surface recombination on $v = 40$
500	1.02×10^6	6.5×10^5	1.17×10^6	1.35×10^6	1.15×10^6	1.06×10^6
1000	6.68×10^5	5.7×10^5	6.79×10^5	1.30×10^6	9.58×10^5	1.03×10^6
1500	5.03×10^5	5.2×10^5	5.45×10^5	1.25×10^6	8.85×10^5	9.9×10^5

[a]Gas-phase kinetics have been included.

model will generate vibrationally active species, which should increase the local temperature and therefore the temperature gradient, as compared with GVS approximation while relaxing in gas phase. In fact, in the latter case, the desorbed molecules are vibrationally cold, and therefore they can be only heated, thus decreasing the local temperature and the gradient. These considerations are supported by the temperature gradients reported in Figs. 5a and 5b. We note, in fact, that DVS and LVS models present higher temperature gradients than with GVS results. These differences disappear when the state-to-state gas-phase kinetics are ignored. These results propagate in the Fourier component of the heat flux that directly depends on the temperature gradient (see Figs. 6a and 6b). As a consequence, the Fourier component decreases passing from the LVS to the GVS models. Note also that the temperature gradient and Fourier component from the DVS overcome the corresponding quantities from the LVS model. This point is always linked to processes in gas-phase kinetics. Molecules in the last vibrational level not only relax, but undergo a privileged dissociation process, thus decreasing the relaxation contribution in the temperature equation. Neglect of state-to-state gas-phase kinetics smooths the differences in the temperature gradient and Fourier component calculated according to the GVS, DVS, and LVS models.

Comparing the diffusion and Fourier components with heat flux, we can observe that they react in an opposite way to the choice of surface model: the diffusion heat flux is higher in the GVS model than in the LVS model. The opposite happens to the Fourier heat flux. As a consequence, the total heat flux depends on the combined effect of its two components, as can be appreciated from Figs. 7a and 7b. When gas-phase kinetics are included (Fig. 7a), the total heat flux

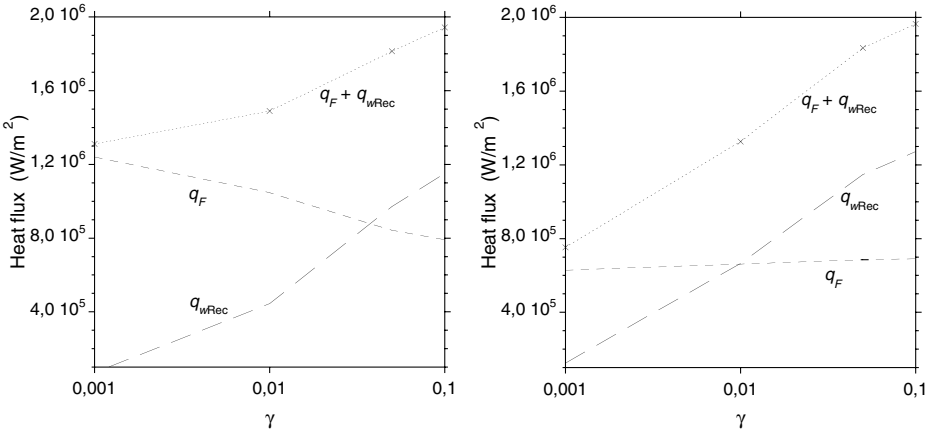

Fig. 8 Heat flux on the surface obtained either a) including or b) neglecting the gas-phase kinetics of Eq. (2). Surface recombination occurs on the first vibrational level (GVS model); $T_w = 300$ K, $T_e = 5950$ K, $P_e = 10^4$ N/m^2, and $\beta = 10^4$ s^{-1}.

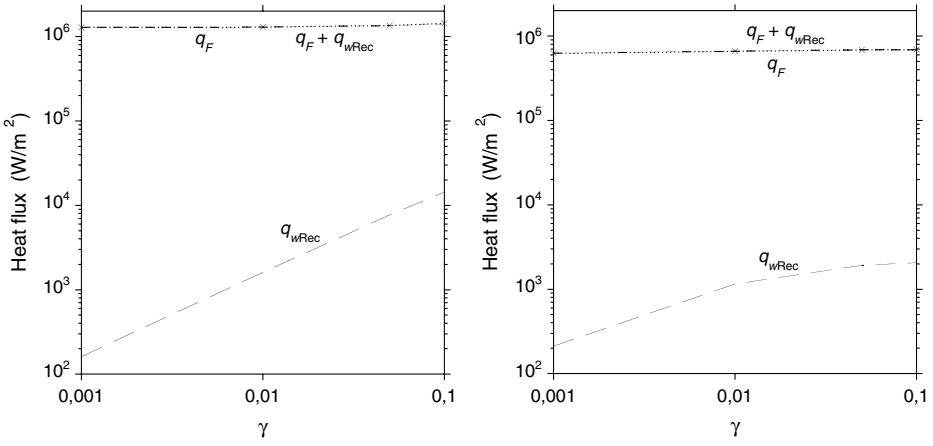

Fig. 9 Heat flux on the surface obtained either a) including or b) neglecting the gas-phase kinetics of Eq. (2). Surface recombination occurs on the last vibrational level (LVS model); $T_w = 300$ K, $T_e = 5950$ K, $P_e = 10^4$ N/m^2, and $\beta = 10^4$ s^{-1}.

Table 3 Values[a] of $q_{wrec} + q_F$ for the NCS, GVS, DVS, and LVS surface recombination models with $T_w = 300$ K, $T_e = 5000$ K, $P_e = 10^3$ N/m^2, $\beta = 5 \times 10^3$ s^{-1}, and $\gamma = 5 \times 10^{-2}$

Model	$q_{wrec} + q_F$, kW/m^2 gas-phase VV and VT processes	$q_{wrec} + q_F$, kW/m^2 gas-phase VV, VT, dissociation, and recombination processes
NCS	114.8 (120.9)[b]	127.7 (123.8–147.6) [b]
GVS	119.3	119.3
DVS	187.9	187.3
LVS	212.9	147.6

[a]The gas-phase dissociation and recombination reactions have been either neglected or included.
[b]The values in parentheses are those calculated by Orsini et al. [2].

calculated by using the LVS model is higher than the corresponding one obtained by the GVS model; that is, the Fourier component prevails in the sum. The practical coincidence of total heat flux calculated according to the GVS and NCS models as a consequence of compensation between diffusive and Fourier contributions should also be noted. The results obtained by neglecting the state-to-state vibrational kinetics (Fig. 7b) rationalize the trends. As expected, the total heat flux decreases from the GVS to the NCS models, passing through the DVS and LVS models; that is, the diffusive terms prevail on the Fourier component. The practical coincidence (Fig. 7b) between the LVS and NCS results in the absence of gas-phase reactions should also be noted.

The results of Fig. 7a can be compared with the corresponding results calculated by Armenise et al. [23] (see Table 2) by using a state-to-state approach for gas-phase kinetics and a macroscopic approach, based on the $Nu/Re^{1/2}$ parameter, for the calculation of the heat transfer on the surface. The gas-phase recombination in the model of [23], which was adopted by our group in the past, is selective: that is, atoms are assumed to recombine either on the vibrational level $v = 45$ or on the vibrational level $v = 25$. Recombination on $v = 45$ approximates the recombination on the top of the vibrational ladder. Recombination on $v = 25$ approximates the recombination on the electronically excited states and, in particular, on the $N_2(A^3\Sigma_u^+)$ state, which immediately relaxes on $v \approx 25$ of the ground state $X^1\Sigma_g^+$.

Results of the two models have been reported in Table 2, showing a qualitative agreement despite the strong differences in the adopted models as well as on the input data. Note, however, that the results of [23] always yield a larger heat flux when the recombination occurs on the $v = 0$ level.

Our $q_F + q_{wrec}$ results are higher when recombination occurs on the last vibrational level as already anticipated and can be rationalized by some qualitative considerations made long ago by Rosner and Feng [24]. These authors stated the possibility of an increase of Fourier component due to the relaxation of the high-lying vibrational levels either in gas phase or on the surface, reporting,

> Surface-catalyzed atom recombination often leads to the formation and desorption of excited molecules. If these "hot" molecules escape the gas mixture layer adjacent to the catalyst without undergoing deexcitation (quenching), the energy transferred to the catalytic surface would clearly be less than if only molecules in local thermodynamic equilibrium (LTE) with the surface were produced and desorbed. However, neglecting spontaneous radiation, excited molecules can be deactivated either by collisions in the gas phase (homogeneous quenching) near the solid surface or by back-reflection and collision with the wall itself (heterogeneous quenching). In either case, their internal energy would be released, perhaps restoring the energy transfer to the surface to near the LTE-value.

Rosner and Feng [24] investigated electronically excited molecules, not vibrationally excited molecules. Nevertheless, they also stated, "If vibrationally excited molecules were produced at surfaces during atom recombination the present formulation would retain many of its present features, however, a more detailed quenching model (accounting for a large number of 'species' of various energy levels) would doubtless be required." These considerations are supported by our calculations without considering gas-phase kinetics, in which the GVS and LVS values follow the expected order: that is, GVS values are higher than LVS values (Fig. 7b).

Let us now examine the heat flux as a function of the recombination coefficient for the two limit cases, GVS and LVS. GVS results have been reported in Figs. 8a and 8b, including and neglecting gas-phase reactions. We can see that the diffusive term increases as γ increases. The reverse is true for the Fourier component. It should also be noted that including gas-phase kinetics for $\gamma > 0.04$, the diffusive term q_{wrec} is higher than the Fourier component q_F. Neglect of gas-phase reactions decreases the Fourier component (Fig. 6b) so that the condition $q_{wrec} > q_F$ occurs for lower values of γ.

Results for the LVS model have been reported in Figs. 9a and 9b. In this case, we note the large predominance of the Fourier component in all of the studied γ range. Moreover, a considerable reduction of the q_{wrec} and q_F components is observed when we neglect gas-phase kinetics (Fig. 9b).

Before ending this section, it is interesting to stress that present results are in close agreement with the results recently reported by Orsini et al. [2] for the noncatalytic surface. In Table 3, the heat transfer calculated according to our NCS, GVS, DVS, and LVS models and calculated by Orsini et al. on a noncatalytic surface have been reported. The input parameters are $T_w = 300$ K, $T_e = 5000$ K, $P_e = 10^3$ N/m^2, $\beta = 5 \times 10^3$ s^{-1}, and $\gamma = 5 \times 10^{-2}$. The gas-phase dissociation and recombination processes have been either

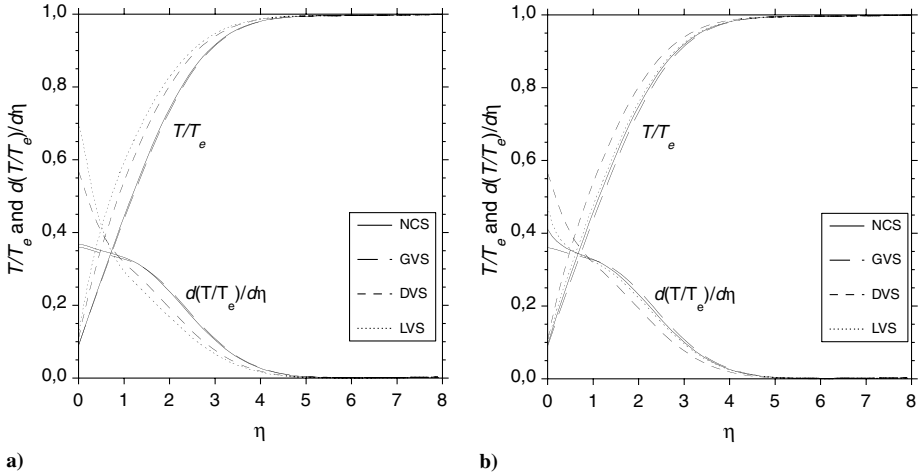

Fig. 10 T/T_e and $\mathrm{d}(T/T_e)/\mathrm{d}\eta$ max profiles along the normal to the surface, η, for the NCS, GVS, DVS, and LVS surface recombination models with $T_w = 300$ K, $T_e = 5000$ K, $P_e = 10^3$ N/m^2, $\beta = 5 \times 10^3$ s^{-1}, and $\gamma = 5 \times 10^{-2}$. The gas-phase dissociation and recombination reactions have been either a) neglected or b) included.

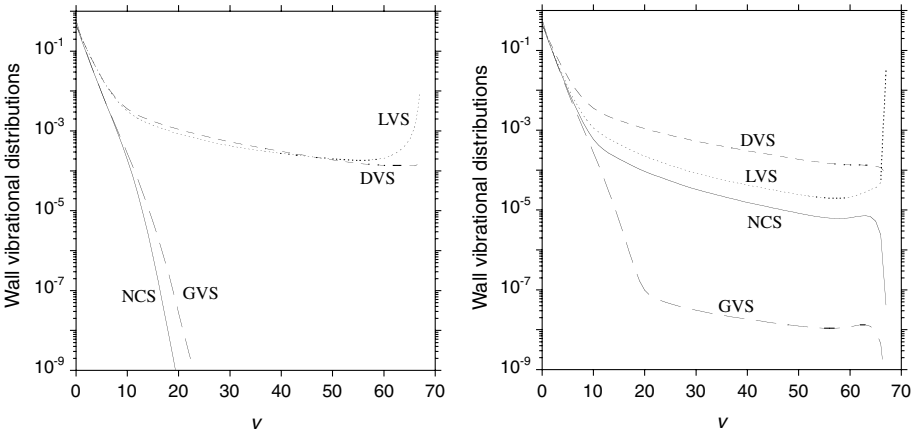

Fig. 11 Surface vibrational distributions versus the vibrational level for the NCS, GVS, DVS, and LVS surface recombination models with $T_w = 300$ K, $T_e = 5000$ K, $P_e = 10^3$ N/m^2, $\beta = 5 \times 10^3$ s^{-1}, and $\gamma = 5 \times 10^{-2}$. The gas-phase dissociation and recombination reactions have been either a) neglected or b) included.

neglected or included. When the gas-phase dissociation and recombination processes have been neglected, our $q_{w\text{rec}} + q_F$ is about 5% lower than the Orsini et al. surface heat flux. When the gas-phase dissociation and recombination processes have been included, our $q_{w\text{rec}} + q_F$ is in the range of the heat flux on the surface calculated by Orsini et al. with different dissociation/recombination models.

When comparing these heat fluxes with those obtained by the previous set of test cases, the dependence of the different heat flux components on the pressure is not easy to understand. In the two sets of test cases, not only the pressure changes, but the external temperature and β change as well. We note, however, by inspecting results at different pressures in the range 10^3–10^5 N/m^2 and keeping the other parameters constant ($T_w = 300$ K, $T_e = 5000$ K, $\beta = 5 \times 10^3$ s^{-1}, and $\gamma = 5 \times 10^{-2}$) that both $q_{w\text{rec}}$ and q_F increase with P_e.

The quantities T/T_e and $\mathrm{d}(T/T_e)/\mathrm{d}\eta$ along the normal to the surface η for the same conditions of Table 3 are reported in Figs. 10a and 10b, respectively, with and without the gas-phase dissociation and recombination reactions. The corresponding vibrational distributions close to the surface are reported in Figs. 11a and 11b. A comparison of these quantities with the corresponding quantities of Orsini et al. [2] for the NCS model again shows a satisfactory agreement.

IV. Conclusions

Different models of diffusive $q_{w\text{rec}}$ and Fourier q_F components of heat transfer on a body under hypersonic flow conditions have been reported and discussed. The models differ on the vibrational level(s) pumped by the heterogeneous recombination process. In particular, two limiting models, the GVS and LVS, are discussed. The first, GVS, considers all the desorbed molecules in the ground vibrational state, and the second, LVS, considers the desorbed molecules in the last vibrational level. A more realistic model, DVS, which considers a spread of the recombination energy in the whole ladder of diatomic molecules, is also discussed. The models have been applied to a N_2–N mixture. The first model, GVS, gives the maximum $q_{w\text{rec}}$ values, and the second model, LVS, gives the minimum $q_{w\text{rec}}$ values. The opposite happens for the Fourier component q_F, so that the total heat transfer ($q_{w\text{rec}} + q_F$) calculated by the GVS model can be lower than that calculated by the LVS model. The results strongly depend on state-to-state gas-phase kinetics. This point stresses the importance of the coupling between heterogeneous and homogeneous state-to-state kinetics in affecting surface heat transfer.

The present results emphasize the role of the vibrational distribution, nascent from heterogeneous recombination, in affecting the heat transfer. The obtained results can be considered only from the qualitative point of view, strongly depending on the assumptions of the selective pumping of the recombination process. Recent MD calculations appear to support the DVS model. Application of the present results to more realistic situations should involve massive use of MD either for the recombination coefficients or for the relaxation coefficients of vibrationally excited molecules on the relevant surface.

Acknowledgment

This paper has been partially supported by ASI (Agenzia Spaziale Italiana) under the CAST (Configurazioni Aerotermodinamiche innovative per Sistemi di Trasporto spaziale) project.

References

[1] Bourdon, A., and Bultel, A., "Numerical Simulation of Stagnation Line Nonequilibrium Airflows for Reentry Applications," *Journal of Thermophysics and Heat Transfer*, Vol. 22, No. 2, 2008, pp. 168–177. doi:10.2514/1.33144

[2] Orsini, A., Rini, P., Taviani, V., Fletcher, D., Kustova, E. V., and Nagnibeda, E. A., "State-to-State Simulation of Nonequilibrium Nitrogen Stagnation-Line Flows: Fluid Dynamics and Vibrational Kinetics," *Journal of Thermophysics and Heat Transfer*, Vol. 22, No. 3, 2008, pp. 390–398. doi:10.2514/1.34545

[3] Park, C., "Review of Chemical-Kinetic Problems of Future NASA Missions, 1: Earth Entries," *Journal of Thermophysics and Heat Transfer*, Vol. 7, No. 3, 1993, pp. 385–398. doi:10.2514/3.431

[4] Doroshenko, V. M., Koudriatsev, N. N., and Smetanin, V. V., "Nonequilibrium Excitation of Internal Molecular Degrees of Freedom in the Shock Layer During Hypersonic Flight," *Shock Waves*, Vol. 2, 1992, pp. 139–146. doi:10.1007/BF01414636

[5] Doroshenko, V. M., Koudriatsev, N. N., Novikov, S. S., and Smetanin, V. V., "Dependence of Heat Transfer on the Formation of Vibrationally Excited Nitrogen Molecules During the Recombination of Atoms in a Boundary Layer," *High Temperature*, Vol. 28, No. 1, 1990, pp. 70–76.

[6] Rutigliano, M., Pieretti, A., Cacciatore, M., Sanna, N., and Barone, V., "N Atoms Recombination on a Silica Surface: A Global Theoretical Approach," *Surface Science*, Vol. 600, No. 18, 2006, pp. 4239–4246. doi:10.1016/j.susc.2005.12.080

[7] Yamamoto, K., Takeuchi, H., and Hyakutake, T., "Scattering Properties and Scattering Kernel Based on the Molecular Dynamics Analysis of Gas-Wall Interaction," *Physics of Fluids*, Vol. 19, No. 8, 2007, Paper 087102. doi:10.1063/1.2770513

[8] Cacciatore, M., Rutigliano, M., and Billing, G. D., "Eley–Rideal and Langmuir-Hinshelwood Recombination Coefficients for Oxygen on Silica Surfaces," *Journal of Thermophysics and Heat Transfer*, Vol. 13, No. 2, 1999, pp. 195–203. doi:10.2514/2.6436

[9] Capitelli, M., Armenise, I., and Gorse, C., "State-to-State Approach in the Kinetics of Air Components Under Re-Entry Conditions," *Journal of Thermophysics and Heat Transfer*, Vol 11, No. 4, 1997, pp. 570–578. doi:10.2514/2.6281

[10] Armenise, I., Esposito, F., and Capitelli, M., "Dissociation-Recombination Models in Hypersonic Boundary Layer Flows," *Chemical Physics*, Vol. 336, No. 1, 2007, pp. 83–90. doi:10.1016/j.chemphys.2007.05.015

[11] Armenise, I., Barbato, M., Capitelli, M., and Kustova, E. V., "State to State Catalytic Models, Kinetics and Transport in Hypersonic Boundary Layers," *Journal of Thermophysics and Heat Transfer*, Vol. 20, No. 3, 2006, pp. 465–476. doi:10.2514/1.18218

[12] Anderson, J. D., Jr., *Hypersonic and High Temperature Gas Dynamics*, McGraw–Hill, Series in Aeronautical and Aerospace Engineering, New York, 1989, pp. 213–259 and 611–636.

[13] Rini, P., Vanden Abeele, D., and Degrez, G., "Elemental Demixing in Inductively Coupled Air Plasma Torches at High Pressures," *Journal of Thermophysics and Heat Transfer*, Vol. 20, No. 1, 2006, pp. 31–40. doi:10.2514/1.15884

[14] Bottin, B., "Aerothermodynamic Model of an Inductively-Coupled Plasma Wind Tunnel," Ph.D. Thesis, Faculte des Sciences Appliquees, Univ. de Liege, and Aeronautics/Aerospace Dept., von Karman Inst. for Fluid Dynamics, Rhode St. Genese, Belgium, 1999.

[15] Kustova, E. V., "On the Simplified State-to-State Transport Coefficients," *Chemical Physics*, Vol. 270, No. 1, 2001, pp. 177–195. doi:10.1016/S0301-0104(01)00352-4

[16] Kustova, E. V., and Nagnibeda, E. A., "Transport Properties of a Reacting Gas Mixture with Strong Vibrational and Chemical Nonequilibrium," *Chemical Physics*, Vol. 233, No. 1, 1998, pp. 57–75. doi:10.1016/S0301-0104(98)00092-5

[17] Armenise, I., Capitelli, M., and Kustova, E. V., "State-to-State Kinetics and Transport Properties of a Reactive Air Flow Near a Re-Entering Body Surface," *Proceedings of the 24th International Symposium on Rarefied Gas Dynamics*, edited by M. Capitelli, American Inst. of Physics, Melville, NY, 2005, pp. 1061–1066.

[18] Hassouni, K., Lombardi, G., Gicquel, A., Capitelli, M., Shakhatov, V. A., and De Pascale, O., "Nonequilibrium Vibrational Excitation of H-2 in Radiofrequency Discharges: A Theoretical Approach Based on Coherent Anti-Stokes Raman Spectroscopy Measurements," *Physics of Plasmas*, Vol. 12, No. 7, 2005, pp. 073301–073310. doi:10.1063/1.1931675

[19] Sharipov, F., "Heat Transfer in the Knudsen Layer," *Physical Review E (Statistical Physics, Plasmas, Fluids, and Related Interdisciplinary Topics)*, Vol. 69, No. 6, 2004, pp. 061201-1–061201-4. doi:10.1103/PhysRevE.69.061201

[20] Sharipov, F., and Kalempa, D., "Velocity Slip and Temperature Jump Coefficients for Gaseous Mixtures 4: Temperature Jump Coefficient," *International Journal of Heat and Mass Transfer*, Vol. 48, No. 6, 2005, pp. 1076–1083. doi:10.1016/j.ijheatmasstransfer.2004.09.035

[21] Méolans, J. G., and Dadzie, S. K., "Wall Temperature Jump in Polyatomic Gas Flows," *Proceedings of the 25th International Symposium on Rarefied Gas Dynamics*, edited by M. S. Ivanov, and A. K. Rebrov, Novosibirsk Univ., Novosibirsk, Russia, 2007, pp. 703–708.

[22] Lifshitz, E. M., and Pitaevskii, L. P., *Physical Kinetics*, Pergamon, Oxford, 1981, p. 51.

[23] Armenise, I., Capitelli, M., Colonna, G., Koudriavtsev, N., and Smetanin, V., "Nonequilibrium Vibrational Kinetics During Hypersonic Flow of a Solid Body in Nitrogen and Its Influence on the Surface Heat Flux," *Plasma Chemistry and Plasma Processing*, Vol. 15, No. 3, 1995, pp. 501–528.

[24] Rosner, D., E., and Feng, H. H., "Energy Transfer Effects of Excited Molecule Production by Surface-Catalyzed Atom Recombination," *Faraday Transactions*, Vol. 70, 1974, pp. 884–907.